A NON-EQUILIBRIUM CLATHRATE HYDRATE DISSOCIATION MODEL AND APPLICATION TO ENCELADUS' PLUME. I. Halevy and S. T. Stewart, Harvard University, Department of Earth and Planetary Sciences, 20 Oxford St., Cambridge, MA 02138 (ihalevy@fas.harvard.edu).

Introduction: Since its detection by the *Cassini* spacecraft in 2005, several explanations have been offered for generation of the plume of water vapor, ice particles and gas jetting from rifts in the south polar terrain (SPT) of Enceladus. The two leading hypotheses are boiling of liquid water [1] and dissociation of clathrate hydrates of mixed gas [2]. The latter, however, has received only rudimentary quantitative treatment, most notably the use of a modified model of equilibrium clathrate hydrate dissociation suitable for terrestrial geologic reservoirs [3]. Dissociation of clathrate hydrates on Enceladus is not an equilibrium process, as the rifts are under tensional stress for only about half of the diurnal cycle [4]. This implies periodic, short term exposure of clathrates to low pressure, alternating with closure of the rifts and an increase in pressure and temperature.

We have constructed a numerical, non-equilibrium clathrate dissociation model suitable for the conditions on Enceladus and perhaps other tectonically active icy bodies. We use the model to show that clathrate hydrate dissociation may explain the plume for a reasonable set of assumptions about the interior structure and composition of Enceladus and about the geometry of the faults. Furthermore, we make predictions of the plume's characteristics during upcoming close approaches to Enceladus and compare these predictions with the values expected if the plume is produced by boiling water, thus providing an observational means of distinguishing between the two major models of the plume.

A Dynamical Clathrate Dissociation Model: Following the numerical approach of Ahmadi *et al.* [5], we have constructed a model to simulate non-equilibrium dissociation of clathrate hydrates on Enceladus. In our model, exposure of clathrates to low pressure destabilizes them, resulting in their dissociation to water ice and a mixture of gases along a "dissociation front". A fraction α of the ice produced by clathrate dissociation becomes entrained in the gas flow and jets out of the rifts together with the gas. The rest of the ice (a fraction $1-\alpha$) is deposited on the fault walls as a porous coating. This ice coating may sublimate from its outer boundary ("sublimation front") at a rate dependent on its temperature. The water vapor produced by sublimation is also entrained in the gas flow, adding to the water content of the escaping plume. The faults may widen or seal, depending on the relative rates of ice sublimation and deposition.

A major difference from preexisting models is that we do not assume equilibrium dissociation of the clathrates. Instead, the temperature in the model domain is computed from the spatial divergence of an energy budget, which is constructed for every model cell. This budget includes conductive, advective and radiative terms, where appropriate, as well as the heat of clathrate dissociation and ice sublimation at the dissociation and sublimation fronts, respectively, if clathrates or ice are out of their field of stability. This way, over the course of a diurnal cycle, the temperature slowly approaches the equilibrium temperature of clathrate dissociation or ice sublimation at the local pressure, rather than being arbitrarily set to it.

We took clathrates to initially exist at any depth where the geothermal temperature is lower than their equilibrium dissociation temperature and higher than the temperature of exsolution to separate solids at the local lithostatic pressure (figure 1). We assumed that the faults do not turn into open chasms when they come under tension, but that they remain constricted with only a few open conduits to the surface. This is consistent with the observation that the plume is composed of a relatively small number of discreet jets [6]. We modeled this as a fraction f_{vent} of the rifts under tension that are actively participating in the venting.

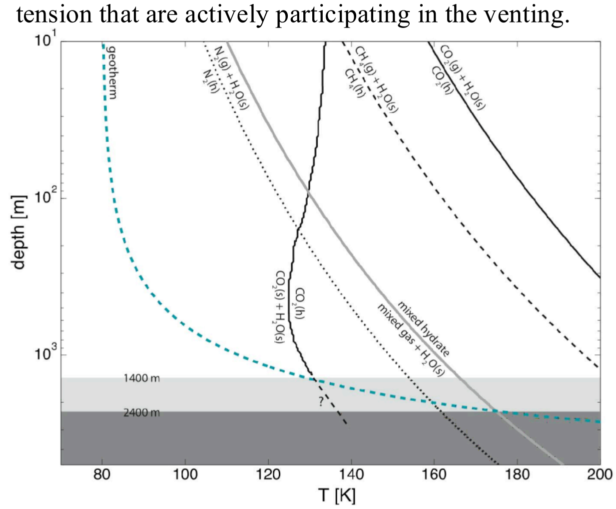

Figure 1: Stability field of clathrate hydrates of N_2, CO_2 and CH_4. The thick gray line denotes a mixture of these clathrates of the composition detected by *Cassini* [10]. The dashed blue line is the geothermal gradient calculated for a surface temperature of 80 K and a surface heat flux of 0.25 W m^{-2} [11].

Results and Discussion: The results of our model depend on the depth of simulation, mainly through the dependence of pressure and temperature on depth. We therefore carried out simulations at variable depth and integrated the fluxes of gas, ice and vapor over an entire column of exposed clathrates. Furthermore, integration over the diurnal cycle is required, since the fraction of "tiger stripes" under tension depends on the orbital position of Enceladus [4] and since the fluxes generated by our model are themselves dependent on the time elapsed since opening of the rifts. We fitted a functional form to the results of Hurford *et al.* [4] for the fraction of rifts under tension as a function of orbital position and were thus able to integrate our results over time.

Figure 2 shows the total mass flux ($F_{total} = F_{water} + F_{gas}$) and the mass ratio of water to gas ($W:G$) as a function of Enceladus' orbital position for venting out of 10% of the rifts under tension ($f_{vent} = 0.1$) and for a gas temperature in the rifts of 150 K. Initial porosity of the ice coating was 50%, consistent with compacted snow [7], since the ice should undergo compaction when the stress in the faults becomes compressional. The porosity of the massive undissociated clathrate was taken to be zero [8]. The figure shows that for this reasonable set of assumptions, the model is able to reproduce the F_{total} (between 140 and 210 kg s^{-1}, based on UVIS stellar occultation measurements [9]) and $W:G$ (~5.7, based on INMS measurements [10]) observed on July 14, 2005. Also marked are the orbital positions during future close approaches to Enceladus, allowing prediction of F_{total} *and* $W:G$ during these encounters if clathrate dissociation is responsible for generation of the plume.

Fitting $W:G$ to past observations required dissociation of clathrates to a depth of ~2600 m, deeper than their maximal depth of stability if the geotherm in the SPT is fully conductive (see figure 1). This may imply that a part of the heat flux is due to advection of warm gas in the rifts and that the temperature in the crust is lower than in the purely conductive case, allowing the existence of clathrates to greater depths.

Finally, our results allow distinction between the boiling liquid and dissociating solid models for generation of the plume. The total mass flux (F_{total}) in both cases depends on exposure of liquid or clathrates to low pressure and is thus expected to resemble in shape the fraction of rifts under tension as a function of orbital position. The water to gas mass ratio ($W:G$), however, should differ between the two scenarios because in the boiling liquid case $W:G$ is an intrinsic property of the liquid reservoir whereas in the clathrate dissociation case it depends on sublimation of the ice coating. This dependence leads to lower $W:G$ as time elapses since the opening of the rifts and the temperature of the walls decreases. Therefore, a measurement of $W:G$ between 3 and 4 during upcoming encounters with Enceladus strengthens the clathrate dissociation model, while a value between 5 and 6, similar to previous measurements, strengthens the boiling water model (see blue arrow in figure 2).

Conclusion: We have presented a non-equilibrium clathrate hydrate dissociation model suitable for the conditions in Enceladus' south polar region. We used the model to explain past observations, showing that clathrate dissociation may produce the observed plume. Finally, we provide an observational means of distinguishing between boiling of a near-surface liquid water reservoir and dissociation of clathrate hydrates as explanations for the plume, by comparing model predictions of the plume's properties to the values expected if liquid water is responsible for its generation.

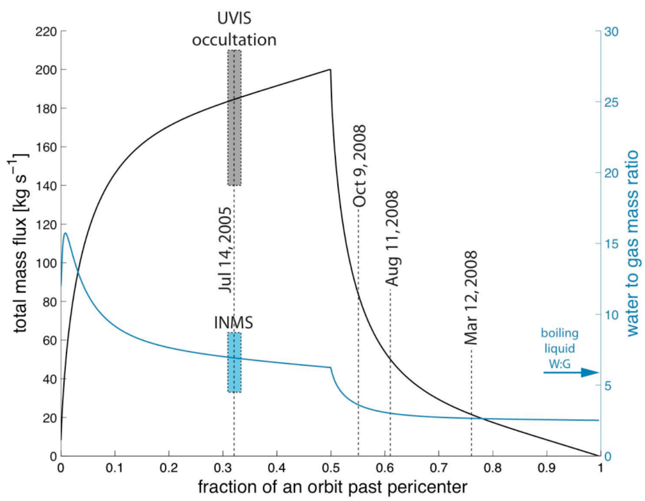

Figure 2: Simulated F_{total} and $W:G$ for the case described in the text are within the range of past observations [9,10]. Future close approaches are marked with dashed vertical lines. The blue arrow marks the expected $W:G$ if boiling liquid is responsible for generation of the plume.

References: [1] Porco C. C. et al. (2006) *Science, 311,* 1393–1401. [2] Kieffer S. W. et al. (2006) *Science, 314,* 1764–1766. [3] Ji C. et al. (2001) *Chem. Eng. Sci.,* 5801–5814. [4] Hurford T. A. et al. (2007) *Nature, 447,* 292–294. [5] Ahmadi G. et al. (2004) *J. Petrol. Sci. Eng., 41,* 269–285. [6] Spitale J. N. and Porco C. C. (2007) *Nature, 449,* 695–697. [7] Baker I. et al. (2007) *Hydrol. Process., 21,* 1624–1629. [8] Schubert G. et al. (2007) *Icarus, 188,* 345–355. [9] Hansen C. J. et al. (2006) *Science, 311,* 1422–1425. [10] Waite J. H. et al. (2006) *Science, 311,* 1419–1422. [11] Spencer J. R. et al. (2006) *Science, 311,* 1401–1405.